



miR-29a-5p Inhibits Prenatal Hair Placode Formation Through Targeting EDAR by ceRNA Regulatory Network

Yao Jiang^{1,2†}, Huatao Liu^{1†}, Quan Zou¹, Shujuan Li¹ and Xiangdong Ding^{1*}

¹National Engineering Laboratory for Animal Breeding, Laboratory of Animal Genetics, Breeding and Reproduction, Ministry of Agriculture, College of Animal Science and Technology, China Agricultural University, Beijing, China, ²Anhui Provincial Key Laboratory of Livestock and Poultry Product Safety Engineering, Institute of Animal Husbandry and Veterinary Medicine, Anhui Academy of Agricultural Sciences, Hefei, China

OPEN ACCESS

Edited by:

De-Li Shi,
Sorbonne University, France

Reviewed by:

Mingxing Lei,
Chongqing University, China
Thomas S. Lisse,
University of Miami, United States

*Correspondence:

Xiangdong Ding
xding@cau.edu.cn

[†]These authors have contributed
equally to this work

Specialty section:

This article was submitted to
Morphogenesis and Patterning,
a section of the journal
Frontiers in Cell and Developmental
Biology

Received: 22 March 2022

Accepted: 28 April 2022

Published: 12 May 2022

Citation:

Jiang Y, Liu H, Zou Q, Li S and Ding X
(2022) miR-29a-5p Inhibits Prenatal
Hair Placode Formation Through
Targeting EDAR by ceRNA
Regulatory Network.
Front. Cell Dev. Biol. 10:902026.
doi: 10.3389/fcell.2022.902026

Hair placode formation is an important stage of hair follicle morphogenesis and it is a complex process facilitated by non-coding RNAs. In this study, we conducted whole transcriptome sequencing analysis of skin, heart, liver, lung, and kidney tissues of day 41 (E41) normal and hairless pig embryos, and respectively detected 15, 8, and 515 skin-specific differentially expressed (DE) lncRNAs, miRNAs, and mRNAs. Furthermore, 18 competing endogenous RNA (ceRNA) networks were constructed. Following weighted gene co-expression network analysis (WGCNA) of stages E39, E41, E45, E52, and E60, between normal and hairless pig embryos, only two ceRNAs (lncRNA2162.1/miR-29a-5p/BMPRI1b and lncRNA627.1/miR-29a-5p/EDAR) that showed period-specific differential expression in E41 skin were retained. Dual-luciferase reporter assays further indicated that EDAR was a direct, functioning target of miR-29a-5p and that no binding site was found in BMPRI1b. Moreover, miR-29a-5p overexpression inhibited the mRNA and protein expression of EDAR while no significant differential expression of BMPRI1b was detected. In addition, over-expressed lncRNA627.1 reduces the expression of miR-29a-5p and increase EDAR expression while inhibits lncRNA627.1 resulted in a opposite expression trend. Cell proliferation result demonstrated that lower expression of EDAR and lncRNA627.1 inhibited hair placode precursor cells (HPPCs) proliferation in a manner similar to that shown by over-expressed miR-29a-5p. This study identified that miR-29a-5p inhibited HPPCs proliferation via the suppression of EDAR expression in the EDA/EDAR signaling pathway, while lncRNA627.1 rescues EDAR expression. Our study provides a basis for a better understanding of the mechanisms underlying the ceRNA complex, miR29a-5p/EDAR/lncRNA627.1, that could regulate hair placode formation, which may help decipher diseases affecting human hair.

Keywords: hair placode formation, ceRNA, miRNA-29a-5p, EDAR, cell proliferation

Abbreviations: BMP2/3/4, bone morphogenetic protein 2/3/4; BMPRI1b, bone morphogenetic protein receptor type 1b; ceRNA, competitive endogenous RNA; CTNNB1, catenin beta 1; DAPI, 6-diamidino-2-phenylindole; DE, differential expression; DKK4, dickkopf WNT signaling pathway inhibitor 4; EDA, ectodysplasin A; EDAR, ectodysplasin A receptor; Edu, 5-ethynyl-20-deoxyuridine; E41, the day of embryo 41; HF, hair follicle; HPPCs, hair placode precursor cells; IF, immunofluorescence; LHX2, LIM homeobox 2; lncRNA, long non-coding RNA; miRNA, microRNA; ncRNA, non-coding RNA; Pc, hair placode; WB, Western blot; WGCNA, weighted gene co-expression network analysis; Wnt10b, Wnt family member 10b.

1 INTRODUCTION

Hair follicle (HF) development is a complex morphogenetic process which occurs in two stages: prenatal hair morphogenesis development, and postnatal hair cycle development (Choi, 2018). Embryonic hair follicle morphogenesis development, which involves mesenchymal and epithelial interactions, begins with the formation of a hair placode in the early epidermis (Duverger and Morasso, 2009; Rishikaysh et al., 2014; Saxena et al., 2019). Therefore, placode formation is key to successful hair follicle morphogenesis. Morphological studies have indicated that hair placodes are formed on day 14.5 (E14.5) in mouse embryos, and during the 12th week [E55–E65 (~E60)] in humans and Cashmere goats (Duverger and Morasso, 2014; Gao et al., 2016). Previous findings of ours have indicated that induction stage of pig hair follicle morphogenesis took place at E41 which the characteristic structure of this stage is hair placode formation (Jiang et al., 2019; Jiang et al., 2021). Thus, in pigs, E41 is the critical point which pig hair follicle morphogenesis begin to develop and hair placode start to form in this point and formation. Placode formation in developing embryonic skin requires stepwise signaling between the epithelial epidermis and the mesenchymal dermis. In recent years, many functional studies have uncovered the essential roles played by major signaling pathways, such as the Wnt/ β -catenin, EDA/EDAR/NF- κ B, and BMP pathways, in placode formation (Rishikaysh et al., 2014; Saxena et al., 2019). Moreover, numerous key genes that play a crucial role in hair placode formation, including *Wnt10b* (Andl et al., 2002), *CTNBN1* (Gay et al., 2015), *LHX2* (Tomann et al., 2016), and *EDA/EDAR* (Zhang et al., 2009) which induce and maintain placode formation, as well as *BMP4* (St-Jacques et al., 1998) and *DKK4* (Fliniaux et al., 2008) which exert inhibitory effects on placode formation, have been identified.

Previous studies were primarily focused on gene function associated with the genetic regulation of placode formation. However, in gene regulation process, whether noncoding RNAs [long noncoding RNA (lncRNA) and microRNAs (miRNA)] are involved by influence gene function at various stages of HF morphogenesis and HF cycling development remains unclear (Andl and Botchkareva, 2015; Ge et al., 2019). Several specific miRNAs that play multiple roles in the regulation of HF development include *miR-22-5p* (Yan et al., 2019a) and *miR-203a-3p* (Luo et al., 2021) in hair follicle stem cells (HFSCs), *miRNA-203* (Ma et al., 2021) and *miR-199a-5p* (Han et al., 2020) in hair follicle development, as well as miR-195-5p in dermal papilla (Zhu et al., 2018), and miR-218-5p in hair shaft growth (Zhao et al., 2019), among others. Furthermore, biogenesis of canonical miRNAs depends on the cytoplasmic processing of pre-miRNAs to mature miRNAs by the Dicer endoribonuclease (Vishlaghi and Lisse, 2020) while Dicer deletion in epidermal result in hair follicle stem cell markers and degenerated (Andl et al., 2006), hair shaft depigmented (Liu et al., 2018a), failure of dermal papilla or hair-follicle maintenance (Teta et al., 2012), a decline in cell proliferation and increased apoptosis in hair follicle (Yi et al., 2006; Yi et al., 2009). In addition, lncRNAs, such as *MSTRG.223165/miR-21/SOX6* in wool HF development (Zhao

et al., 2020), as well as *lncRNA5322/miR-19b-3p/MAPK1* (Cai et al., 2019) and *XR_310320.3/chi-miR-144-5p/HOXC8* (Ma et al., 2019) in hair follicle stem cells (HFSCs), also act as competitive endogenous RNAs (ceRNAs) to sponge miRNA and relieve the inhibitory effects exerted by these miRNAs on target genes during the regulation of HF development. Although the role of ncRNAs in HF development has been gradually deciphered, molecular mechanisms underlying the role played by ncRNAs, particularly the ceRNA regulatory networks, in the formation and maintenance of placodes remain unclear. Although a few studies have revealed that *lncRNA2437* (Yue et al., 2016), *miRNA195* (Liu et al., 2018b) and *XLOC297809* (Nie et al., 2018) are involved in hair follicle initiation and placode induction, the genetic mechanisms underlying these processes have not yet been elucidated. A previous study of ours showed that hairless pigs were mainly caused by the blockage of hair placode formation at E41 in induction stage of pig hair follicle morphogenesis (Jiang et al., 2019). However, the precise molecular basis of blocked hair placode formation in pigs remains elusive, while the role of miRNA and lncRNA in hair placode formation remains unexplored as well.

Therefore, the objective of the current study was to screen out key candidate ceRNAs which may exert significant effects on hair placode formation *via* whole-transcriptome sequencing. Different tissues (skin, heart, liver, lung, and kidney) at E41 and different periods (E39, E41, E45, E52, and E60) in skin were sequenced to screened tissue- and periods-specific expression RNAs at E41 skin. Furthermore, the ceRNA based regulatory mechanism underlying hair placode formation was verified at the cellular level. Thus, our study of pig models should enhance future exploration of the hitherto unrecognized role played by the ceRNA network in hair placode formation in humans.

2 MATERIALS AND METHODS

2.1 Ethics Approval

All animal procedures were evaluated and authorized by Institutional Animal Care and Use Committee (IACUC). The whole procedure for samples collected was carried out in strict accordance with the protocol approved by the IACUC at the China Agricultural University. The IACUC of the China Agricultural University specifically approved this study (permit number DK996).

2.2 Animals and Phenotype

E41 is a crucial stage for prenatal placode formation during hair follicle morphogenesis. In this study, tissues, including skin, heart, liver, lung, spleen, and kidney, from hairless ($n = 3$) and normal ($n = 3$) pig embryos at day 41 of gestation (E41). One embryo each from a litter, were sampled. In addition, mRNA sequencing of skin from hairless ($n = 3$) and normal ($n = 3$) embryos, one each from a litter, were also sampled at days 39 (E39), 45 (E45), 52 (E52), and 60 (E60) of gestation. The phenotype of every sample was identified following Hematoxylin and Eosin (HE) staining (**Supplementary Figure S1**). Hair follicle density was measured and those embryos with

less than one hair follicle per cm^2 and larger than four hair follicles per cm^2 were determined as hairless and normal, respectively (Jiang et al., 2019).

2.3 RNAs (mRNA and ncRNA) Sequencing and Analysis

Total RNA was extracted using Trizol reagent (Invitrogen, Carlsbad, CA, United States), according to the manufacturer's instructions. Quantity and purity were analyzed using a Bioanalyzer 2,100 and an RNA 6,000 Nano Labchip Kit (Agilent, Palo Alto, CA). Only RNA samples with suitable RNA electrophoresis results ($28\text{S}/18\text{S} \geq 1.0$) and RNA integrity number (RIN) ≥ 7.5 could be analyzed further. The skin, heart, liver, lung and kidney tissues of normal ($n = 3$) and hairless ($n = 3$) embryos from the same litter were selected for mRNA, lncRNA and miRNA sequencing at E41. Embryo skins (normal = 3, hairless = 3) from the other four periods, namely E39, E45, E52, and E60, were selected for mRNA sequencing. mRNA and lncRNA were sequenced on Illumina HiSeq 4,000 and miRNA on HiSeq 2,000 platforms, which generated 150-bp paired-end and 50-bp single-end reads, respectively. Differentially expressed (DE) ncRNAs and mRNAs were identified using HISAT2 (Kim et al., 2019) and DESeq2 (Love et al., 2014) with an adjusted p value (false discovery rate, FDR) < 0.05 and a $\log_2|\text{FoldChange}| > 1$.

2.3.1 mRNA Sequence Analysis

An Illumina high-throughput platform was used for mRNA sequencing and raw data was obtained using FastQC v0.11.9 (Chen et al., 2017). Quality control of the raw reads was conducted using NGSQtoolkit_v2.3.3 (Patel and Jain, 2012). The *Sus scrofa* 11.1 reference genome (http://ftp.ensembl.org/pub/release-104/fasta/sus_scrofa/dna/Sus_scrofa.SsCrofa11.1.dna.toplevel.fa.gz) and gene sets file (http://ftp.ensembl.org/pub/release-104/gtf/sus_scrofa/Sus_scrofa.SsCrofa11.1.104.gtf.gz) were downloaded from Ensembl. HISAT2 (v2.0.4) and StringTie (v1.3.1) (Pertea et al., 2016) were performed to obtain clean reads aligned to the reference genome and mRNA reads were assembled for each sample. DESeq2 (Love et al., 2014) package was used for differential gene expression analysis.

2.3.2 lncRNA-Seq Analysis

Quality control and mapping methods of lncRNA-seq data were similar to those used for mRNA-seq data. Candidate lncRNAs were selected using the following conditions: 1) Transcript length ≥ 200 and exon number ≥ 2 , and Fragments Per Kilobase per Million reads (FPKM) > 0.5 ; 2) Minimal read coverage ≥ 3 in at least one sample; 3) Filter known non-lncRNA annotations; and 4) Classify selected candidate lncRNAs, using the following four tools to predict coding potential: CPC2 (Kang et al., 2017), CNCI (Sun et al., 2013), PhyloCSF (v20121028) (Lin et al., 2011), and Pfam Scan databases (Finn et al., 2016). DESeq2 package was used to identify differentially expressed lncRNA between different groups at $p_{\text{adj}} < 0.05$. The lncRNA function depends on protein coding genes *via cis* and *trans* acting elements. *Cis*-acting (in which lncRNAs act on adjacent genes within a

100 kb distance) and *trans*-acting (in which the Pearson correlation of mutual expression levels is ≥ 0.95 or ≤ -0.95) are widely adopted to forecast lncRNA gene interactive pairs. Bedtools (Quinlan and Hall, 2010) was used to identify neighboring genes approximately 100 kb upstream and downstream of differentially upregulated and downregulated lncRNAs, respectively.

2.3.3 microRNA-Seq Analysis

Quality control methods used for miRNA-seq data were similar to those used for mRNA-seq data, where an NGSQtoolkit_v2.3.3 was used. BWA software (Tam et al., 2015) was used for mapping and pig reference miRNA. Novel miRNA was predicted *via* miRDeep2 (Friedlander et al., 2012). The DESeq2 package was performed to identify miRNAs that were differentially expressed between different groups and a screening threshold for identifying differentially expressed miRNA was established at $p_{\text{adj}} < 0.05$. The target genes of miRNAs were predicted using Target Scan (http://www.targetscan.org/mamm_31/), RNA hybrid (<https://biserv.cebitec.uni-bielefeld.de/rnahybrid/>) and miRWalk v3.0 database (<http://mirwalk.umm.uni-heidelberg.de/>). Google charts (<https://developers.google.com/chart/>) were used to illustrate the targeting relationship between miRNA and mRNA. GO and Pathway enrichment analysis was performed using g:Profiler (<https://biit.cs.ut.ee/gprofiler/gost>) and ToppGene (<https://toppgene.cchmc.org/enrichment.jsp>), which terms with a adjusted p value (false discovery rate, FDR) greater than 0.05 were filtered.

2.4 Integrated ceRNA Regulatory Network

To investigate the role and interactions between ncRNAs and mRNAs during HF morphogenesis, ceRNA regulatory networks were constructed. The targeted relationships between lncRNA and miRNA were predicted *via* miRanda. Next, regulatory networks of lncRNA–miRNA–mRNA pairs were constructed based on co-location and co-expression (Tay et al., 2014). Two expression trend models, namely lncRNA downregulated | miRNA upregulated | mRNA downregulated (lncRNA–|miRNA+|mRNA–) and lncRNA upregulated | miRNA downregulated | mRNA upregulated (lncRNA+|miRNA–|mRNA+) were used to establish ceRNA regulatory networks. All networks were graphically displayed using Cytoscape3.6 (Shannon et al., 2003).

2.5 Weighted Gene Co-Expression Network Analysis

The mRNA sequencing of 30 embryo skins from five different stages (WGCNA_skins_periods; E39, E41, E45, E52, and E60) of normal and hairless pigs were integrated into the gene expression matrix for WGCNA. Then mRNA-seq data, which contained the expression data of 14,555 genes and 15,160 genes (Sum counts > 10) for WGCNA_E41_tissues and WGCNA_skins_periods, was used to construct the gene expression matrix. Variance stabilizing transformation (VST) (Anders and Huber, 2010) function in the DESeq2 package was used to normalize and transform the two

gene expression matrices respectively. The construction of two gene co-expression networks was based on the WGCNA package (Pei et al., 2017). Gene co-expression networks must conform to scale-free characteristics and obey power law distribution. Following sensitivity analysis of scale-free topology, the soft threshold power parameters of the two networks were set at 10 and 12, respectively (Ravasz et al., 2002).

2.6 Cell Culture

Approximately 2 cm² skin samples from the lateral backsides of the pig embryo at days 41 gestation were surgically removed following standard, aseptic procedures. The tissues were cut at the interface of the sub cutaneous adipose layer and dermis. The remaining tissues were sub merged in 0.25% dispase II (Gibco, Grand Island, United States) overnight at 4°C to separate the epidermis from the dermis, following which the epidermis was cut into small blocks of approximately 1 mm³ in size, which were used as explants to culture hair placode precursor cells (HPPCs). The culture medium [DMEM (Gibco, Grand Island, United States) was supplemented with 10% FBS (Gibco, Grand Island, United States) and 1% penicillin-streptomycin (Gibco, Grand Island, United States)]. Normally, FBCs grew from each explant approximately 5 days after initial adhesion and were passaged when they reached 100% confluency. Typically, FBCs from the 3rd passage were used for all experiments. Human embryonic kidney (HEK)-293T (National Biomedical Cell Collection, Beijing, China) were cultured for Dual-Luciferase assay in DMEM supplemented with 10% FBS. All cells were incubated at 37°C in a 5% CO₂.

2.7 Transfections

FBCs were seeded at 3×10^5 cells per well in a 12-well plate and grown for 12 h. Then, the cells were transfected with 50 pmol of negative control of *ssc-miR-29a* mimics (mimics-NC, $n = 3$), *ssc-miR-29a* mimics ($n = 3$), 100 pmol of negative control of *ssc-miR-29a* inhibitor (inhibitor-NC, $n = 3$) or *ssc-miR-29a* inhibitor ($n = 3$), and 20 pmol of negative control EDAR siRNA (EDAR-NC, $n = 3$) or EDAR siRNA ($n = 3$), using Lipofectamine 3,000 (Invitrogen, Carlsbad, CA, United States) according to the manufacturer's instructions. The mimics and inhibitor were designed and synthesized by RIBOBIO (Guangzhou, China). Total RNA and protein were isolated from the transfected cells 48/72 h post-transfection for further analysis.

2.8 Cell Proliferation Assay

Cell proliferation was assessed using a CCK-8 Cell Counting kit (Beyotime, Shanghai, China). FBCs were seeded in a 96-well plate (2×10^3 cells per well) and then cultured for 12, 24, 36, 48, 60, or 72 h before adding 10 μ l of CCK-8 (5 mg/ml) to the culture medium in each well. After incubating for 2 h, absorbance at 450 nm was measured using a Thermo-max microplate (ThermoFisher, Massachusetts, United States) reader. All experiments involving each transfection were performed in triplicate. HPPCs were transferred to culture medium with 50 μ M 5-ethynyl-20-deoxyuridine (Edu, Beyotime, Beijing, China) for 2 h at 37°C after 36 h transfection. Afterwards, cells were fixed in 4% paraformaldehyde for 15 min at room

temperature (RT), and then permeabilized with 0.3% Triton X-100 for 10 min. To block non-specific binding, cells were incubated in blocking buffer (PBS containing 3% bovine serum albumin, 0.3% Triton X-100) for 1 h at room temperature. Next, the cells were incubated with a solution containing 10 mM Edu for 30 min in the dark. Nuclei were stained with 10 μ g/ml 4, 6-diamidino-2-phenylindole (DAPI, Solarbio, Beijing, China) solution in the dark for 10 min. A Leica SP8 confocal microscope was used to capture three randomly selected fields to visualize the number of Edu-stained cells.

2.9 Immunofluorescence Staining

Cells were fixed in 4% paraformaldehyde for 15 min after 48 h transfection and then permeabilized in 0.3% Triton X-100 for 10 min. Subsequently, cells were blocked with blocking solution (3% BSA, 0.3% Triton X-100, 10% FBS complemented with PBS) for 2 h. Then, immunofluorescence staining was performed using anti-EDAR (ABclonal, Guangzhou, China; 1:200) overnight at 4°C. Next, cells were stained with Alexa 594-labeled anti-rabbit antibody (Antgene, Wuhan, China; 1:200) for 1 h. Cell nuclei were visualized using DAPI (Solarbio, Beijing, China) solution in darkness for 10 min. Three randomly selected images were used to perform analysis.

2.10 Western Blotting

Western blotting (WB) was used to detect protein quantity. In brief, the sample was lysed in RIPA lysis solution, to extract total protein, and denatured. Next, the sample proteins were separated via SDS-PAGE gel electrophoresis under conditions involving a constant voltage of 100 V. In this study, the proteins were transferred from SDS-PAGE gel to PVDF membranes using a semi-dry transfer method. Then the membranes were blocked for 4 h, and incubated with primary antibodies against EDAR (ABclonal, 1:2000) and BMPRIb (ABclonal, 1:1500) overnight at 4°C. Next, the membranes were washed thrice with TBST (Trisbuffered saline) and incubated with secondary antibodies (1:1200 dilution) at room temperature for 1.5 h. Finally, a BeyoECL plus kit (Beyotime) was used to detect the protein signal. GAPDH (ABclonal, 1:1500) was used as a reference protein and blots were analyzed using IPWIN software.

2.11 Quantitative RT-PCR Analysis

Total RNA was isolated from dorsal pig skin with TriZol (Invitrogen, SanDiego, CA) following the manufacturer's instructions. Next, cDNA was reverse transcribed using a PrimeScriptTM RT reagent kit with gDNA Eraser (Takara, Kyoto, Japan). RT-PCR was performed with LightCycler 480 SYBR Green I Master (Roche, Mannheim, Germany) mix on a LightCycler 480 real-time PCR system. GAPDH was used as a normalized control and relative gene expression was calculated based on the $2^{-\Delta\Delta CT}$ formula. Measurements were recorded in triplicate. The following PCR conditions used: 95°C "hot start" for 10 min; 35 cycles of 95°C for 10 s, 60°C for 10 s, and 72°C for 10 s; and 72°C for 5 min. Primer sequences are provided (**Supplementary Table S3**). Differences between the gene expression of normal and hairless pigs were measured via a t test.

TABLE 1 | The summarizes of DE mRNAs and ncRNAs in skin, heart, liver, lung and kidney of normal and hairless pig embryos at E41.

mRNA/ncRNA	Expression	Skin	Heart	Liver	Lung	Kidney
mRNA	Upregulated	372	96	298	288	231
	Downregulated	299	227	122	51	70
	Total	671	323	423	339	301
lncRNA	Upregulated	2	3	22	5	8
	Downregulated	13	9	6	19	12
	Total	15	12	28	24	20
miRNA	Upregulated	9	36	13	0	3
	Downregulated	0	18	0	1	0
	Total	9	54	13	1	3

3 RESULTS

A summary of the descriptive statistics of lncRNA-seq, miRNA-seq, and mRNA-seq data pertaining to different tissues, indicating the relatively high-quality of transcriptome data in this study is shown (**Supplementary Table S1**). Furthermore, mRNA and ncRNA (lncRNA and miRNA) sequencing of skin, heart, liver, lung, and kidney tissues of three normal and three hairless pig embryos at E41 stage were performed, and the number of differentially expressed (DE) mRNAs and ncRNAs are shown (**Table 1**). The DE RNAs (mRNAs, miRNAs, and lncRNAs) are illustrated in detail (**Supplementary Figure S2**) and sample-to-sample correlation in the five tissues was high (**Supplementary Figure S2**).

3.1 Specific Differential Expression of mRNA and ncRNAs in Pig Embryos Skin at E41

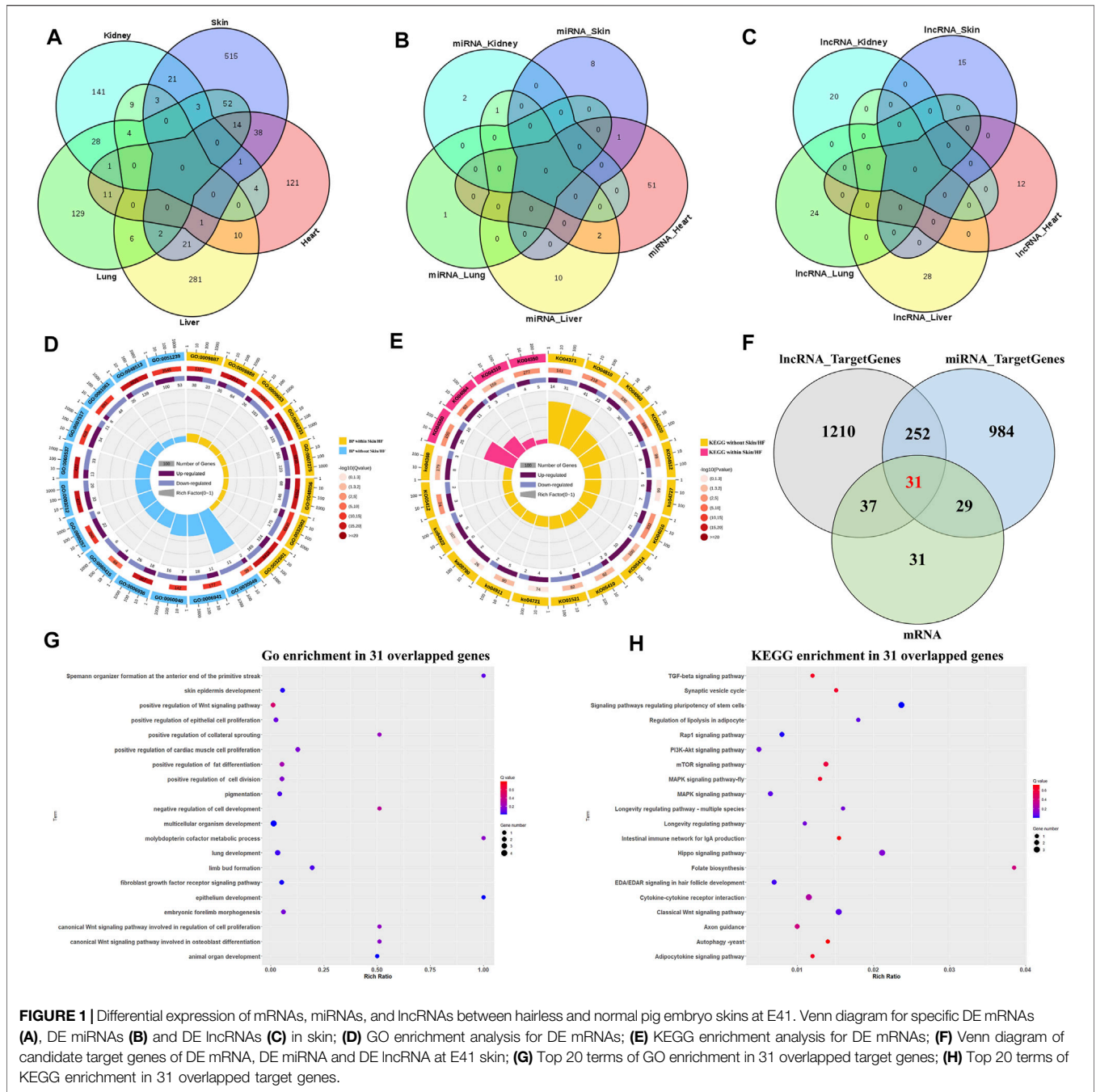
Overlap between DE mRNAs, DE miRNAs and DE lncRNAs are illustrated (**Figures 1A–C**). In addition, 515 DE mRNAs (**Figure 1A**), 8 DE miRNAs (**Figure 1B**), and 15 DE lncRNAs (**Figure 1C**) were specifically differentially expressed between E41 skins of hairless and normal embryos. Next, qRT-PCR indicated that expression levels of randomly selected DE mRNA and ncRNA transcripts were highly consistent (**Supplementary Figure S3**), indicating the reliability of our RNA-seq data. Eight GO terms (**Figure 1D**) of the 515 DE mRNAs were significantly enriched in *skin development* and *epidermal development and differentiation*, while four hair follicle related signaling pathways, including the *Wnt* signaling pathway and the *BMP* signaling pathway, were identified (**Figure 1E**). Based on GO and pathway enrichment analysis, 128 of the 515 DE mRNAs (**Supplementary Table S2**) were selected which play important roles in HF development and hair placode formation. A total of 1,530 *cis* or *trans* target genes were predicted for the 15 DE lncRNAs in skin (**Table 1**), and among that, 68 target genes overlapped with those for the 128 DE mRNAs (**Supplementary Figure S4A**). Similarly, 1296 overlapped target genes were predicted for the 8 DE miRNAs by miRanda (3,452 target genes) and RNAhybrid (4,507 target genes); (**Supplementary Figure S4B**). Furthermore, *epithelium development*, the *Wnt*

signaling pathway, the *EDA/EDAR signaling pathway*, and the *BMP signaling pathway*, among others, were enriched in these overlapped target genes (**Supplementary Figures S3D,F**), of which 60 genes overlapped with those of 128 DE mRNAs (**Figure 1F**; **Supplementary Figure S4C**). Thirty-one genes that overlapped between normal and hairless pig embryos at E41 stage skin tissue were identified based on DE mRNAs and target genes of DE miRNAs and lncRNAs (**Figure 1F**). These were enriched in hair follicle development, including *skin epidermis development* and *epithelial cell differentiation* (**Figure 1G**). Similarly, enriched KEGG pathways included the classical HF morphogenesis pathways such as the *Wnt*, *TGF- β* , and *EDA/EDAR signaling pathways* (**Figure 1H**). As well, the key genes *EDAR*, *DKK4*, *BMPR1B*, *BMP3*, *WNT3*, and *FGFR2*, among others, were identified.

3.2 Construction and Weighted Gene Co-Expression Network Analysis of ceRNA Regulatory Networks

Based on expression trend models (lncRNA–|miRNA+| mRNA–) pertaining to the expression trends of 31 overlapping target genes as well as the lncRNAs and miRNAs regulating the expression of these genes, 18 ceRNA regulatory networks were constructed. These networks contained 18 overlapped DE genes, five DE lncRNAs, and three DE miRNAs (**Figure 2A**). Function and pathway enrichment analysis of GO (**Figure 2B**) showed that *EDAR*, *FGFR2*, *BMPR1b*, and *VANGL1* were enriched in classical hair follicle pathways, such as *Wnt*, *EDAR/NF- κ B*, *TGF- β* , *BMP*, and *FGF signaling pathways*, and that the GO terms were mainly related to *skin morphology and formation*, *hair and skin development function* and *fibroblast cell line differentiation*.

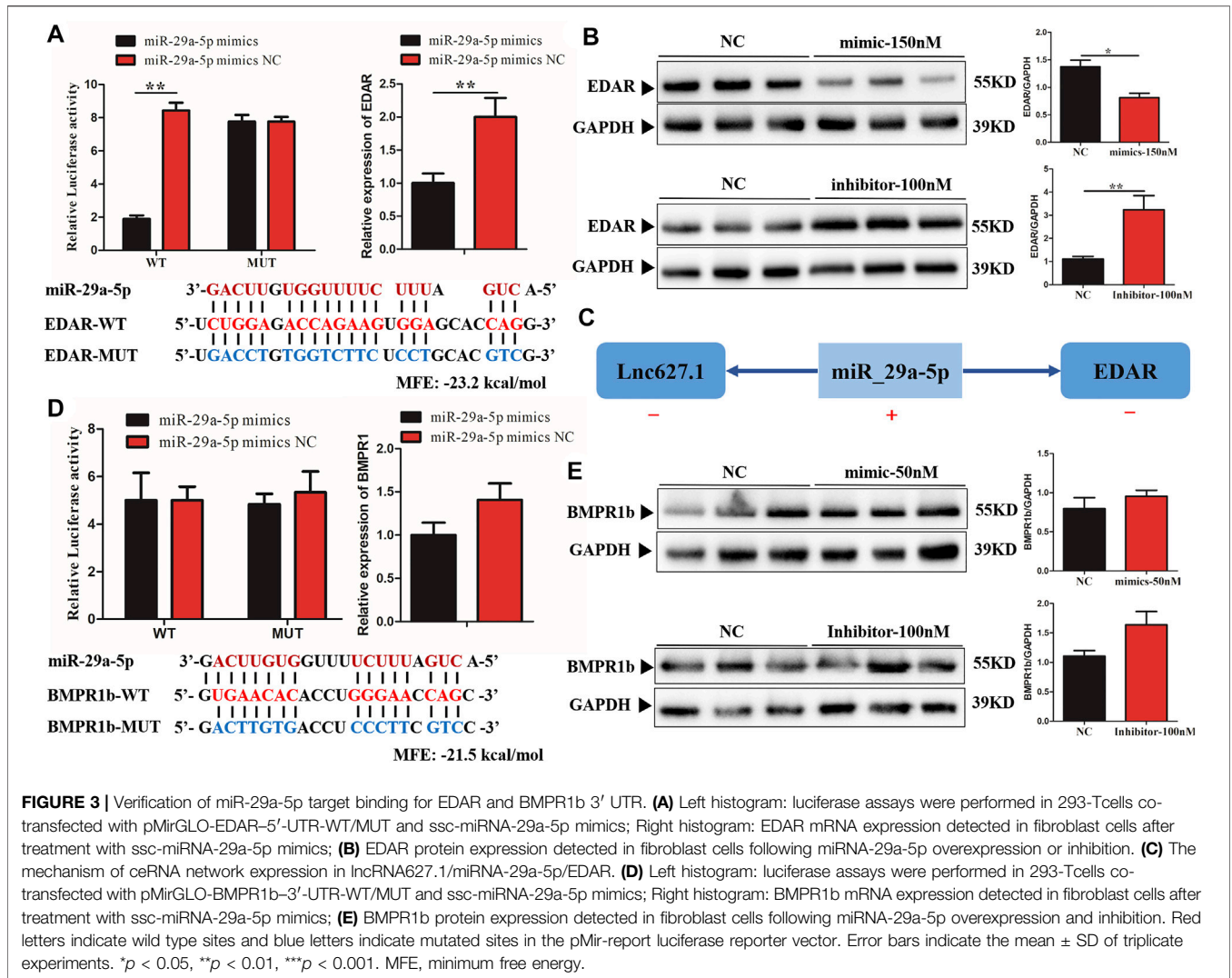
To further screen ceRNAs for skin-specific expression at E41, WGCNA was performed on normal and hairless pig skin at five stages, namely E39, E41, E45, E52, and E60, using mRNA sequencing. The independence degree approximated 0.8 while the average connectivity degree was higher (**Supplementary Figures S4A,C**). In total, 24 and 28 distinct gene co-expression modules were constructed for the normal group and the hairless group, respectively (**Supplementary Figures S4B,D**). Modules showing $p < 0.05$ at E41 were selected, and interestingly, four modules, *MEbrown* ($p = 0.03$), *MEgreen* ($P = 4E-04$), *MEpink* ($p = 0.03$) and *MEgray* ($p = 0.0083$), were identified in normal pigs (**Figure 2C**), while no significant module was found in hairless pigs (**Supplementary Figure S6**). Among the hub genes of the four significant modules, only *EDAR* (**Figure 2D**) and *BMPR1b* (**Figure 2E**), of the 18 DE target genes in ceRNA, were found to be involved. Additionally, both *EDAR* and *BMPR1b* were interacted with many hub genes (such as *KRT5*, *WNT8A*, and *KRT4*) which were related to hair follicle development, in the most significant *MEgreen* module (**Figure 2D**). Moreover, the expression levels of *EDAR* (**Figures 1A, 2F**) and *BMPR1b* (**Figures 1A, 2G**) in skin at different periods, were found to be not only tissue-specific but also period-specific at E41 ($p < 0.001$). Therefore, two ceRNAs,



lncRNA2162.1/miR-29a-5p/BMPR1b and lncRNA627.1/miR-29a-5p/EDAR, were retained. The results of *ssc-miR-29a-5p* sequence alignment in different species revealed that *ssc-miR-29a-5p* is highly conserved among species (Figure 2H), suggesting the importance of the role played by *ssc-miR-29a-5p*. A previous study of ours indicated that E41 constituted the critical stage of hair placode formation, and the results of our current study indicated that *EDAR* and *BMPR1b* may play an important role in hair placode formation *via* the ceRNA network.

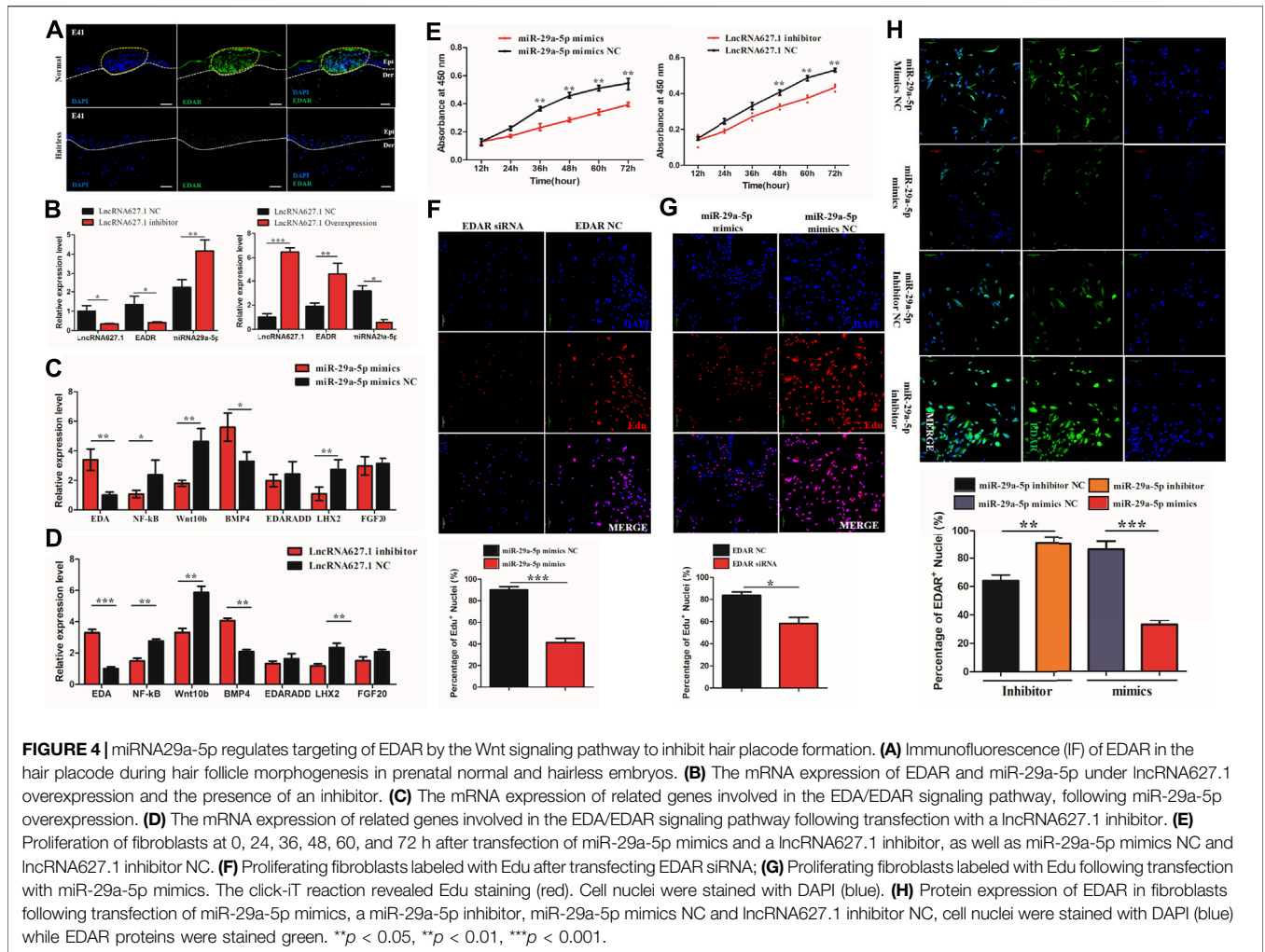
3.3 EDAR Was a Target Gene of miR-29a-5p in ceRNA

Among the ceRNAs, only *miR-29a-5p* was able to regulate *EDAR* and *BMPR1b*. In order to validate direct regulation of the expression levels of *EDAR* and *BMPR1b* by *miR-29a-5p*, a construct containing the 5'UTR of the potential target genes, or the sequence with the mutant seed region, was co-transfected together with *miR-29a-5p* mimics in human 293T cells. As predicted, *miR-29a-5p* mimics significantly reduced EDAR-WT-5'UTR ($p < 0.01$) luciferase activity, whereas no



and *miR-29a-5p* was upregulated (Figure 4B). To gain further insights into how lncRNA627.1 and *miR-29a-5p* regulate EDAR, related genes, *EDA*, *NF- κ B*, *Wnt10b*, *BMP4*, *EDARADD*, *LHX2*, and *FGF20*, associated with the EDA/EDAR signaling pathway, were also detected after transfecting HPPCs with *miR-29a-5p* mimics and a lncRNA627.1 inhibitor. Among the *miR-29a-5p* mimics group, *BMP4* ($p < 0.05$) was remarkably upregulated while *EDA* ($p < 0.01$), *NF- κ B* ($p < 0.01$), *Wnt10b* ($p < 0.01$) and *LHX2* ($p < 0.01$) were significantly downregulated (Figure 4C). Similar results were also observed in the lncRNA627.1 inhibitor group (Figure 4D). Our results demonstrated that the similar expression trend in EDAR related genes by lncRNA627.1 expression inhibition and *miR-29a-5p* overexpression which suggested that a regulation might existed between lncRNA627.1 and *miR-29a-5p* and need furthermore investigation to explore whether regulated by ceRNA (Figures 4C,D). In addition, proliferation of HPPCs further confirmed the regulation by *miR-29a-5p* and lncRNA627.1. Thirty-six h following the transfection of *miR-29a-5p* mimics and lncRNA627.1 inhibitor, the number of viable cells in the

miR-29a-5p mimics group was significantly decreased ($p < 0.01$), and continued to decrease further for 48, 60, and 72 h, a result consistent with findings for the lncRNA627.1 inhibitor group (Figure 4E). We further explored the role played by the association between EDAR and *miR-29a-5p* in HPPCs proliferation, via siRNA-mediated EDAR silencing as well as via *miR-29a-5p* mimics mediated suppression of EDAR expression. Edu staining assays indicated that following the reduction of EDAR expression, the proportion of Edu⁺ HPPCs cells were reduced when transfected with EDAR siRNA ($p < 0.001$) (Figure 4F) or *miR-29a-5p* mimics ($p < 0.05$) (Figure 4G). Meanwhile, compared with that of mimics/inhibitor NC groups, EDAR⁺ HPPCs cells were upregulated following transfection *miR-29a-5p* inhibitor ($p < 0.01$), while it was downregulated in the *miR-29a-5p* mimics group ($p < 0.001$) (Figure 4H). Considered together, our results indicated that *miRNA29a-5p* inhibits HPPCs proliferation by suppressing the expression of the targeting gene, EDAR, in the EDA/EDAR signaling pathway, while lncRNA627.1 removes such inhibition.



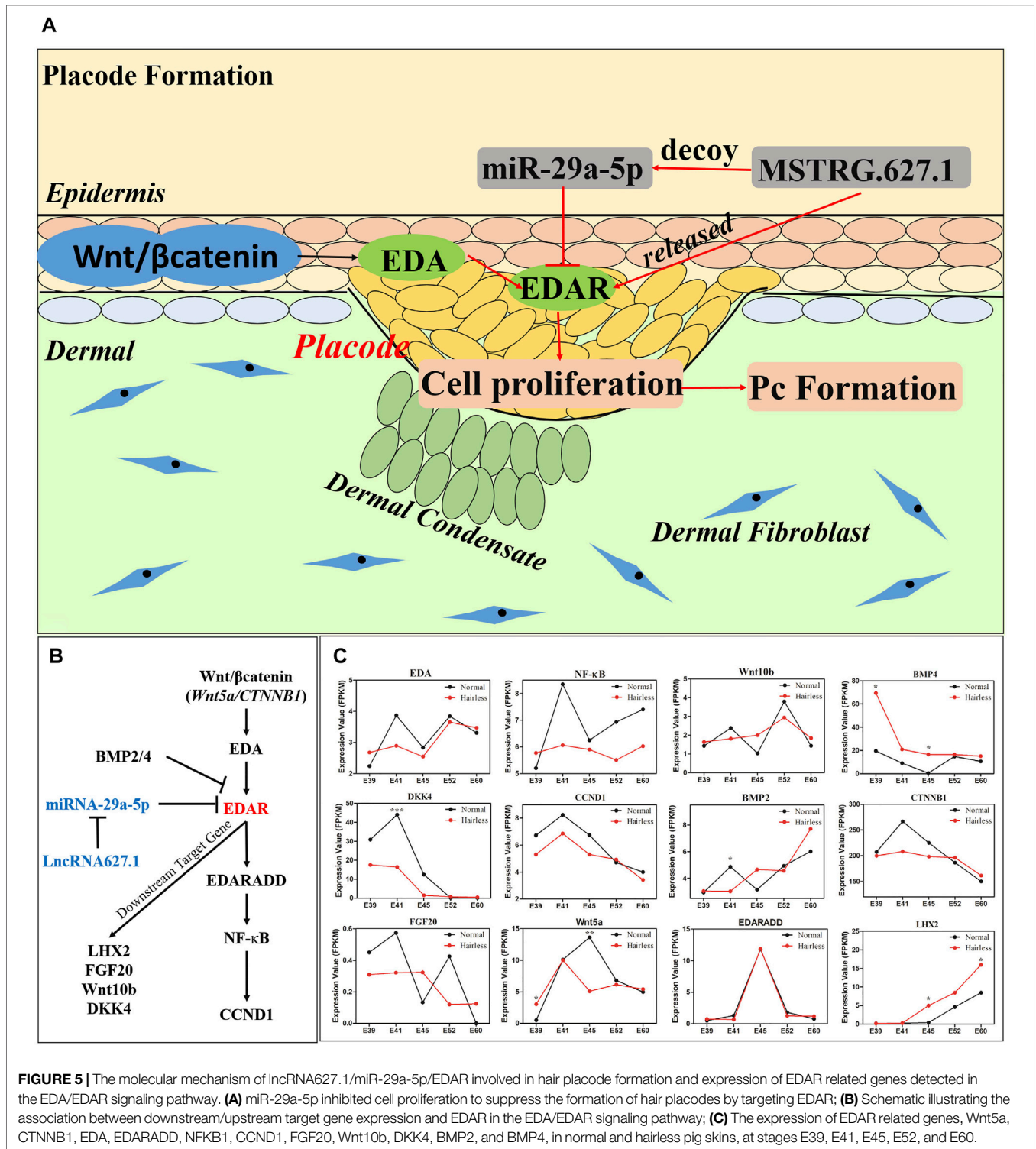
4 DISCUSSION

Previous studies of ours (Jiang et al., 2019) indicated that impairment of hair placode formation at E41 constitutes the main cause of hairlessness in hairless pigs. In this study, whole transcriptome sequencing (mRNA, lncRNA, and miRNA) of normal and hairless pig embryos at E41 screened out *EDAR* and an associated regulatory mechanism involving ceRNAs. Of the known key genes involved in hair placode formation, *EDAR* appears to play an important, early role by regulating signaling molecules involved in the establishment, formation, and regulation of placodes (Saxena et al., 2019). High expression levels of *EDAR* increased the number and size of hair placodes (Mustonen et al., 2004; Mohri et al., 2008) whereas hair placode formation could neither be induced nor maintained in the absence of *EDAR* (Schmidt-Ullrich et al., 2006; Fliniaux et al., 2008). Impaired hair placode formation was associated with a reduction in the epidermal expression levels of *EDAR*, *Lef1*, and *Shh*, which are essential for hair follicle morphogenesis (Mohri et al., 2008).

In our study, *EDAR* was highly expression at the hair placodes of normal skin while no expression in hairless (Figure 4A) which

not only confirmed the key role of *EDAR* in hair placode formation, but also showed consistency with the results of previous studies (Schmidt-Ullrich et al., 2006; Zhang et al., 2009; Wu et al., 2020). Furthermore, this study also demonstrated that high *EDAR* expression promotes the proliferation of HPPCs, while low *EDAR* expression inhibits such proliferation (Figure 4F). Previous studies had also reported that *EDAR* exerts its effect on epithelial (Jaskoll et al., 2003) and matrix progenitor cell proliferation (Wang et al., 2017a) via the EDA/EDAR/NF-κB signaling pathway. In hair follicles, *Gata6* regulates the rapid proliferation of epithelial (matrix) progenitors during adult mouse hair follicle regeneration, by stimulating the activation of *EDAR* and NF-κB pathways (Wang et al., 2017a). Furthermore, *EDAR* and NF-κB play a role in keratinocyte proliferation and hair placode down-growth (Schmidt-Ullrich et al., 2006).

Besides that, it was necessary to use HPPCs in this study, due to the absence of a specific cell line that could be utilized for hair placode formation research. Although, it is advantageous to use tissue block culture and organoid culture methods to detect hair follicle related phenotype at the cellular level while still exist many problems. In tissue block culture for hair placode, the culture



environment and culture additive such as activator, enzymes, small molecules, growth factors are still unknown in pig [Zhou et al. (2018), Yan et al. (2019b)] while the combination selection of multiple cell lines and precises space culture environment limit the development of organoid culture (Lee et al., 2018; Lee et al., 2020; Lee and Koehler, 2021). HPPCs at the E41 stage were used

in this study because another research of us (unpublished) found that the formation of hair placode mainly comes from a kind of hair placode precursor cell (HPPCs) in epidermal (Supplementary Figure S7A), which not only specifically expresses EDAR, but also highly expresses fibroblast cells related marker genes (*COL1A1*, *LUM*, *Vimentin*), just similar

to a pseudo fibroblast cell lineage (**Supplementary Figure S7B**). We speculated that these pseudo fibroblasts (HPPCs) might be the key cells leading to the formation of hair placode which could also be screened from epidermal tissue and highly expressed FB marker, *Vimentin* and *LUM* (**Supplementary Figure S7C**). Thus, these results were the main basis for us to select HPPCs to research in this study. In addition, according to Chen *et al.*, fibroblast proliferation plays a functional role in hair placode initiation (Chen *et al.*, 2012) while proliferation capacity was the determining factor in the initiation of placode formation (Duverger and Morasso, 2009; Schneider *et al.*, 2009; Rishikaysh *et al.*, 2014). Our study provided a speculation which EDAR could directly promote hair placode development *via* a pseudo fibroblasts lineage, HPPCs cells proliferation.

Increasingly, evidence indicates that ncRNA participates in the regulation of hair follicle morphogenesis and development *via* the ceRNA network which imposes mutual regulation among miRNAs, lncRNAs, and mRNAs (Cai *et al.*, 2019; Zhao *et al.*, 2020). According to ceRNA theory, miRNA suppresses gene expression by recognizing specific target mRNAs, while lncRNAs, which act as natural miRNA sponges, inhibit miRNA function and modulate the expression of target mRNAs by interacting with miRNA response elements (Salmena *et al.*, 2011). In our study, significantly high expression levels of *miR-29a-5p* suppressed the expression of *EDAR* and *lncRNA627.1* in hairless pig skin tissue at E41 (**Figure 2B**). Meanwhile, overexpression of *lncRNA627.1* elevated the expression of *EDAR* while the expression of *miR-29a-5p* was reduced which suggested that *lncRNA627.1* may disrupt the binding between miRNA and mRNA while competitive binding displacement assay was needed in further investigation (**Figure 4B**). Another similar regulatory mechanism based on ceRNAs is that of *miR-144-5p*, which indirectly affects HFSCs by targeting *lncRNA310320.3* and *lncRNA311077.2* (Ma *et al.*, 2019). *lncRNA679* promoted *Wnt3* expression by targeting *miR-221-5p* in hair follicle cycle development (Wang *et al.*, 2017b). Generally, ncRNA function involves regulation of the expression of targeted mRNAs (Salmena *et al.*, 2011; Tay *et al.*, 2014); for example, *lncRNA5322* serves as a ceRNA of *miR-19b-3p* to elevate *MAPK1* expression, ultimately promoting proliferation of HFSCs and epidermal regeneration in mouse models (Cai *et al.*, 2019). Previous studies have reported that *miR-29a* plays a positive role in skin fibroblast protection (Zhou *et al.*, 2016), hair follicle regeneration (Zhu *et al.*, 2020), and HFSC proliferation (Guo *et al.*, 2018; Ge *et al.*, 2019) by regulating target genes. The results of the current study further revealed that *miR-29a-5p* plays a role in placode formation by regulating *EDAR*, where *miR-29a-5p* downregulated *EDAR* expression, thereby inhibiting HPPCs proliferation and hair placode formation. In contrast, *lncRNA627.1* upregulated *EDAR* expression by suppressing *miR-29a-5p* expression (**Figure 5A**). It's worth noting that current data supported a model where *lncRNA627.1* acts upstream of *miR-29a* expression (**Figures 4B–E**), but no direct evidence that *lncRNA627.1* could release the *EDAR* expression by competitively binding *miR-29a-5p* based on ceRNA

regulatory mechanism. Thus, the relation between *lncRNA627.1* and *miR-29a-5p*, such as competitive binding displacement assay, needs to be further verification.

According to previous studies, a complex regulatory mechanism involving multiple genes and pathways underlies hair placode formation (Duverger and Morasso, 2009; Schneider *et al.*, 2009; Sennett and Rendl, 2012). Besides *lncRNA627.1/miR-29a-5p/EDAR*, we also identified other DE mRNAs at E41, such as *BMP3* (Nie *et al.*, 2018), *DKK4* (Mokry and Pisal, 2020), *FGFR2* (Nguyen *et al.*, 2018), and *FRZB* (Hu *et al.*, 2020), which participate in hair placode formation *via* the *Wnt/β-catenin*, *BMP* and *FGF* signaling pathways (**Supplementary Table S2**). Although excluded from ceRNA construction, these were differentially expressed between normal and hairless pigs at E41, suggesting these genes may exert a synergistic effect on hair placode formation *via* other regulatory mechanisms.

EDAR influences hair placode formation *via* its participation in the *EDA/EDAR* signaling pathway (Schmidt-Ullrich *et al.*, 2006). Therefore, we constructed an interaction network of *EDAR*-related genes based on previous reports (Fliniaux *et al.*, 2008; Zhang *et al.*, 2009; Wu *et al.*, 2020); (**Figure 5B**), and detected the expressions of these genes at E39, E41, E45, E52 and E60 stages of normal and hairless pig embryo skins (**Figure 5C**). The expression trends of *EDA*, *NF-κB*, *Wnt10b* and *BMP4* were consistent with their expression in HPPCs, in which *EDAR* expression was inhibited by *miR-29a-5p* and *lncRNA627.1* (**Figures 4C,D**). Reportedly, *EDA* (Zhang *et al.*, 2009), *Wnt10b* (Andl *et al.*, 2002), and *NF-κB* (Schmidt-Ullrich *et al.*, 2006) were required for the initiation of hair placodes by the *EDA/EDAR* signaling pathway, while *BMP4* acted as an inhibitor for *EDAR* (Rishikaysh *et al.*, 2014). On the other hand, the differences between the expression levels of some *EDAR* related genes (**Figure 5C**) at E41, were not significant (**Figure 5B**), and this may be attributed to heterogeneity of skin cells (Takahashi *et al.*, 2020) and spatio-temporal gene expression. Our findings not only revealed the importance of *EDAR* in hair placode formation, but also the role played by multi-gene co-regulation which is exerted *via* participation of the *EDAR* signaling pathway in hair placode formation. However, further research on molecular communication between the multiple genes involved in co-regulation is needed.

DATA AVAILABILITY STATEMENT

The datasets presented in this study can be found in online repositories. The names of the repository/repositories and accession number(s) can be found below: <https://ngdc.cncb.ac.cn/>, CRA004672.

ETHICS STATEMENT

The animal study was reviewed and approved by Institutional Animal Care and Use Committee of the China Agricultural University.

AUTHOR CONTRIBUTIONS

YJ performed research and wrote the paper; HL performed bioinformatics analysis; QZ and SL performed sample collection and prepared biological samples; XD designed the research and revised the paper; and all authors read and approved the final manuscript.

FUNDING

This work was supported by grants for the National Natural Science Foundation of China (32070568, 31671327); the National Key Research and Development Project (2019YFE0106800), China Agriculture Research System of MOF and MARA

REFERENCES

- Anders, S., and Huber, W. (2010). Differential Expression Analysis for Sequence Count Data. *Genome Biol.* 11 (10), R106. doi:10.1186/gb-2010-11-10-r106
- Andl, T., and Botchkareva, N. V. (2015). MicroRNAs (miRNAs) in the Control of HF Development and Cycling: the Next Frontiers in Hair Research. *Exp. Dermatol* 24 (11), 821–826. doi:10.1111/exd.12785
- Andl, T., Murchison, E. P., Liu, F., Zhang, Y., Yunta-Gonzalez, M., Tobias, J. W., et al. (2006). The miRNA-Processing Enzyme Dicer Is Essential for the Morphogenesis and Maintenance of Hair Follicles. *Curr. Biol.* 16 (10), 1041–1049. doi:10.1016/j.cub.2006.04.005
- Andl, T., Reddy, S. T., Gaddapara, T., and Millar, S. E. (2002). WNT Signals Are Required for the Initiation of Hair Follicle Development. *Dev. Cell* 2 (5), 643–653. doi:10.1016/s1534-5807(02)00167-3
- Cai, B., Wang, X., Liu, H., Ma, S., Zhang, K., Zhang, Y., et al. (2019). Up-regulated lncRNA5322 Elevates MAPK1 to Enhance Proliferation of Hair Follicle Stem Cells as a ceRNA of microRNA-19b-3p. *Cell Cycle* 18 (14), 1588–1600. doi:10.1080/15384101.2019.1624111
- Chen, D., Jarrell, A., Guo, C., Lang, R., and Atit, R. (2012). Dermal β -catenin Activity in Response to Epidermal Wnt Ligands Is Required for Fibroblast Proliferation and Hair Follicle Initiation. *Development* 139 (8), 1522–1533. doi:10.1242/dev.076463
- Chen, S., Huang, T., Zhou, Y., Han, Y., Xu, M., and Gu, J. (2017). AfterQC: Automatic Filtering, Trimming, Error Removing and Quality Control for Fastq Data. *BMC Bioinforma.* 18 (Suppl. 3), 80. doi:10.1186/s12859-017-1469-3
- Choi, B. (2018). Hair-Growth Potential of Ginseng and its Major Metabolites: A Review on its Molecular Mechanisms. *Ijms* 19 (9), 2703. doi:10.3390/ijms19092703
- Duverger, O., and Morasso, M. I. (2009). Epidermal Patterning and Induction of Different Hair Types during Mouse Embryonic Development. *Birth Defect Res. C* 87 (3), 263–272. doi:10.1002/bdrc.20158
- Duverger, O., and Morasso, M. I. (2014). To Grow or Not to Grow: Hair Morphogenesis and Human Genetic Hair Disorders. *Seminars Cell & Dev. Biol.* 25–26, 22–33. doi:10.1016/j.semcdb.2013.12.006
- Finn, R. D., Coggill, P., Eberhardt, R. Y., Eddy, S. R., Mistry, J., Mitchell, A. L., et al. (2016). The Pfam Protein Families Database: towards a More Sustainable Future. *Nucleic Acids Res.* 44 (D1), D279–D285. doi:10.1093/nar/gkv1344
- Fliniaux, I., Mikkola, M. L., Lefebvre, S., and Thesleff, I. (2008). Identification of Dkk4 as a Target of Eda-A1/Edar Pathway Reveals an Unexpected Role of Ectodysplasin as Inhibitor of Wnt Signalling in Ectodermal Placodes. *Dev. Biol.* 320 (1), 60–71. doi:10.1016/j.ydbio.2008.04.023
- Friedländer, M. R., Mackowiak, S. D., Li, N., Chen, W., and Rajewsky, N. (2012). miRDeep2 Accurately Identifies Known and Hundreds of Novel microRNA Genes in Seven Animal Clades. *Nucleic Acids Res.* 40 (1), 37–52. doi:10.1093/nar/gkr688
- Gao, Y., Wang, X., Yan, H., Zeng, J., Ma, S., Niu, Y., et al. (2016). Comparative Transcriptome Analysis of Fetal Skin Reveals Key Genes Related to Hair Follicle

(CARS-35), China Postdoctoral Science Foundation (2020M681977).

ACKNOWLEDGMENTS

The authors gratefully acknowledge the colleagues in the molecular quantitative genetics team of China Agricultural University for their helpful comments on the manuscript.

SUPPLEMENTARY MATERIAL

The Supplementary Material for this article can be found online at: <https://www.frontiersin.org/articles/10.3389/fcell.2022.902026/full#supplementary-material>

- Morphogenesis in Cashmere Goats. *PLoS One* 11 (3), e0151118. doi:10.1371/journal.pone.0151118
- Gay, D. L., Yang, C.-C., Plikus, M. V., Ito, M., Rivera, C., Treffeisen, E., et al. (2015). CD133 Expression Correlates with Membrane Beta-Catenin and E-Cadherin Loss from Human Hair Follicle Placodes during Morphogenesis. *J. Investigative Dermatology* 135 (1), 45–55. doi:10.1038/jid.2014.292
- Ge, M., Liu, C., Li, L., Lan, M., Yu, Y., Gu, L., et al. (2019). miR-29a/b1 Inhibits Hair Follicle Stem Cell Lineage Progression by Spatiotemporally Suppressing WNT and BMP Signaling. *Cell Rep.* 29 (8), 2489–2504. doi:10.1016/j.celrep.2019.10.062
- Guo, L., Huang, X., Liang, P., Zhang, P., Zhang, M., Ren, L., et al. (2018). Role of XIST/miR-29a/LIN28A Pathway in Denatured Dermis and Human Skin Fibroblasts (HSFs) after Thermal Injury. *J. Cell. Biochem.* 119 (2), 1463–1474. doi:10.1002/jcb.26307
- Han, W., Yang, F., Wu, Z., Guo, F., Zhang, J., Hai, E., et al. (2020). Inner Mongolian Cashmere Goat Secondary Follicle Development Regulation Research Based on mRNA-miRNA Co-analysis. *Sci. Rep.* 10 (1), 4519. doi:10.1038/s41598-020-60351-5
- Hu, X., Zhang, X., Liu, Z., Li, S., Zheng, X., Nie, Y., et al. (2020). Exploration of Key Regulators Driving Primary Feather Follicle Induction in Goose Skin. *Gene* 731, 144338. doi:10.1016/j.gene.2020.144338
- Jaskoll, T., Zhou, Y.-M., Trump, G., and Melnick, M. (2003). Ectodysplasin Receptor-Mediated Signaling Is Essential for Embryonic Submandibular Salivary Gland Development. *Anat. Rec.* 271A (2), 322–331. doi:10.1002/ar.a.10045
- Jiang, Y., Jiang, Y., Zhang, H., Mei, M., Song, H., Ma, X., et al. (2019). A Mutation in MAP2 Is Associated with Prenatal Hair Follicle Density. *FASEB J.* 33 (12), 14479–14490. doi:10.1096/fj.201901187R
- Jiang, Y., Zou, Q., Liu, B., Li, S., Wang, Y., Liu, T., et al. (2021). Atlas of Prenatal Hair Follicle Morphogenesis Using the Pig as a Model System. *Front. Cell Dev. Biol.* 9, 721979. doi:10.3389/fcell.2021.721979
- Kang, Y.-J., Yang, D.-C., Kong, L., Hou, M., Meng, Y.-Q., Wei, L., et al. (2017). CPC2: a Fast and Accurate Coding Potential Calculator Based on Sequence Intrinsic Features. *Nucleic Acids Res.* 45 (W1), W12–W16. doi:10.1093/nar/gkx428
- Kim, D., Paggi, J. M., Park, C., Bennett, C., and Salzberg, S. L. (2019). Graph-based Genome Alignment and Genotyping with HISAT2 and HISAT-Genotype. *Nat. Biotechnol.* 37 (8), 907–915. doi:10.1038/s41587-019-0201-4
- Lee, J., Böske, R., Tang, P.-C., Hartman, B. H., Heller, S., and Koehler, K. R. (2018). Hair Follicle Development in Mouse Pluripotent Stem Cell-Derived Skin Organoids. *Cell Rep.* 22 (1), 242–254. doi:10.1016/j.celrep.2017.12.007
- Lee, J., and Koehler, K. R. (2021). Skin Organoids: A New Human Model for Developmental and Translational Research. *Exp. Dermatol* 30 (4), 613–620. doi:10.1111/exd.14292
- Lee, J., Rabbani, C. C., Gao, H., Steinhart, M. R., Woodruff, B. M., Pflum, Z. E., et al. (2020). Hair-bearing Human Skin Generated Entirely from Pluripotent Stem Cells. *Nature* 582 (7812), 399–404. doi:10.1038/s41586-020-2352-3

- Lin, M. F., Jungreis, I., and Kellis, M. (2011). PhyloCSF: a Comparative Genomics Method to Distinguish Protein Coding and Non-coding Regions. *Bioinformatics* 27 (13), i275–i282. doi:10.1093/bioinformatics/btr209
- Liu, X., Zhang, P., Ji, K., Zhang, J., Yang, S., Du, B., et al. (2018a). Cyclin-dependent Kinase 5 Regulates MAPK/ERK Signaling in the Skin of Mice. *Acta Histochem.* 120 (1), 15–21. doi:10.1016/j.acthis.2017.10.009
- Liu, Z., Yang, F., Zhao, M., Ma, L., Li, H., Xie, Y., et al. (2018b). The Intragenic mRNA-microRNA Regulatory Network during Telogen-Anagen Hair Follicle Transition in the Cashmere Goat. *Sci. Rep.* 8 (1), 14227. doi:10.1038/s41598-018-31986-2
- Love, M. I., Huber, W., and Anders, S. (2014). Moderated Estimation of Fold Change and Dispersion for RNA-Seq Data with DESeq2. *Genome Biol.* 15 (12), 550. doi:10.1186/s13059-014-0550-8
- Luo, Z., Dou, J., Xie, F., Lu, J., Han, Q., Zhou, X., et al. (2021). miR -203a-3p Promotes Loureirin A-Induced Hair Follicle Stem Cells Differentiation by Targeting Smad1. *Anat. Rec.* 304 (3), 531–540. doi:10.1002/ar.24480
- Ma, S., Wang, Y., Zhou, G., Ding, Y., Yang, Y., Wang, X., et al. (2019). Synchronous Profiling and Analysis of mRNAs and ncRNAs in the Dermal Papilla Cells from Cashmere Goats. *BMC Genomics* 20 (1), 512. doi:10.1186/s12864-019-5861-4
- Ma, T., Li, J., Li, J., Wu, S., Ba, X., Jiang, H., et al. (2021). Expression of miRNA-203 and its Target Gene in Hair Follicle Cycle Development of Cashmere Goat. *Cell Cycle* 20 (2), 204–210. doi:10.1080/15384101.2020.1867789
- Mohri, Y., Kato, S., Umezawa, A., Okuyama, R., and Nishimori, K. (2008). Impaired Hair Placode Formation with Reduced Expression of Hair Follicle-Related Genes in Mice Lacking *Igr4*. *Dev. Dyn.* 237 (8), 2235–2242. doi:10.1002/dvdy.21639
- Mokry, J., and Pisal, R. (2020). Development and Maintenance of Epidermal Stem Cells in Skin Adnexa. *Ijms* 21 (24), 9736. doi:10.3390/ijms21249736
- Mustonen, T., Ilmonen, M., Pummila, M., Kangas, A. T., Laurikkala, J., Jaatinen, R., et al. (2004). Ectodysplasin A1 Promotes Placodal Cell Fate during Early Morphogenesis of Ectodermal Appendages. *Development* 131 (20), 4907–4919. doi:10.1242/dev.01377
- Nguyen, M. B., Cohen, I., Kumar, V., Xu, Z., Bar, C., Dauber-Decker, K. L., et al. (2018). FGF Signalling Controls the Specification of Hair Placode-Derived SOX9 Positive Progenitors to Merkel Cells. *Nat. Commun.* 9 (1), 2333. doi:10.1038/s41467-018-04399-y
- Nie, Y., Li, S., Zheng, X., Chen, W., Li, X., Liu, Z., et al. (2018). Transcriptome Reveals Long Non-coding RNAs and mRNAs Involved in Primary Wool Follicle Induction in Carpet Sheep Fetal Skin. *Front. Physiol.* 9, 446. doi:10.3389/fphys.2018.00446
- Patel, R. K., and Jain, M. (2012). NGS QC Toolkit: a Toolkit for Quality Control of Next Generation Sequencing Data. *PLoS One* 7 (2), e30619. doi:10.1371/journal.pone.0030619
- Pei, G., Chen, L., and Zhang, W. (2017). WGCNA Application to Proteomic and Metabolomic Data Analysis. *Methods Enzymol.* 585, 135–158. doi:10.1016/bs.mie.2016.09.016
- Perteira, M., Kim, D., Perteira, G. M., Leek, J. T., and Salzberg, S. L. (2016). Transcript-level Expression Analysis of RNA-Seq Experiments with HISAT, StringTie and Ballgown. *Nat. Protoc.* 11 (9), 1650–1667. doi:10.1038/nprot.2016.095
- Quinlan, A. R., and Hall, I. M. (2010). BEDTools: a Flexible Suite of Utilities for Comparing Genomic Features. *Bioinformatics* 26 (6), 841–842. doi:10.1093/bioinformatics/btq033
- Ravasz, E., Somera, A. L., Mongru, D. A., Oltvai, Z. N., and Barabási, A.-L. (2002). Hierarchical Organization of Modularity in Metabolic Networks. *Science* 297 (5586), 1551–1555. doi:10.1126/science.1073374
- Rishikaysh, P., Dev, K., Diaz, D., Qureshi, W., Filip, S., and Mokry, J. (2014). Signaling Involved in Hair Follicle Morphogenesis and Development. *Ijms* 15 (1), 1647–1670. doi:10.3390/ijms15011647
- Salmena, L., Poliseno, L., Tay, Y., Kats, L., and Pandolfi, P. P. (2011). A ceRNA Hypothesis: the Rosetta Stone of a Hidden RNA Language? *Cell* 146 (3), 353–358. doi:10.1016/j.cell.2011.07.014
- Saxena, N., Mok, K. W., and Rendl, M. (2019). An Updated Classification of Hair Follicle Morphogenesis. *Exp. Dermatol.* 28 (4), 332–344. doi:10.1111/exd.13913
- Schmidt-Ullrich, R., Tobin, D. J., Lenhard, D., Schneider, P., Paus, R., and Scheidereit, C. (2006). NF- κ B Transmits Eda A1/EdaR Signalling to Activate Shh and Cyclin D1 Expression, and Controls Post-initiation Hair Placode Down Growth. *Development* 133 (6), 1045–1057. doi:10.1242/dev.02278
- Schneider, M. R., Schmidt-Ullrich, R., and Paus, R. (2009). The Hair Follicle as a Dynamic Miniorgan. *Curr. Biol.* 19 (3), R132–R142. doi:10.1016/j.cub.2008.12.005
- Sennett, R., and Rendl, M. (2012). Mesenchymal-epithelial Interactions during Hair Follicle Morphogenesis and Cycling. *Seminars Cell & Dev. Biol.* 23 (8), 917–927. doi:10.1016/j.semcdb.2012.08.011
- Shannon, P., Markiel, A., Ozier, O., Baliga, N. S., Wang, J. T., Ramage, D., et al. (2003). Cytoscape: a Software Environment for Integrated Models of Biomolecular Interaction Networks. *Genome Res.* 13 (11), 2498–2504. doi:10.1101/gr.1239303
- St-Jacques, B., Dassule, H. R., Karavanova, I., Botchkarev, V. A., Li, J., Danielian, P. S., et al. (1998). Sonic Hedgehog Signaling Is Essential for Hair Development. *Curr. Biol.* 8 (19), 1058–1069. doi:10.1016/s0960-9822(98)70443-9
- Sun, L., Luo, H., Bu, D., Zhao, G., Yu, K., Zhang, C., et al. (2013). Utilizing Sequence Intrinsic Composition to Classify Protein-Coding and Long Non-coding Transcripts. *Nucleic Acids Res.* 41 (17), e166. doi:10.1093/nar/gkt646
- Takahashi, R., Grzenda, A., Allison, T. F., Rawnsley, J., Balin, S. J., Sabri, S., et al. (2020). Defining Transcriptional Signatures of Human Hair Follicle Cell States. *J. Investigative Dermatology* 140 (4), 764–773. e764. doi:10.1016/j.jid.2019.07.726
- Tam, S., Tsao, M.-S., and McPherson, J. D. (2015). Optimization of miRNA-Seq Data Preprocessing. *Briefings Bioinforma.* 16 (6), 950–963. doi:10.1093/bib/bbv019
- Tay, Y., Rinn, J., and Pandolfi, P. P. (2014). The Multilayered Complexity of ceRNA Crosstalk and Competition. *Nature* 505 (7483), 344–352. doi:10.1038/nature12986
- Teta, M., Choi, Y. S., Okegbe, T., Wong, G., Tam, O. H., Chong, M. M. W., et al. (2012). Inducible Deletion of Epidermal Dicer and Drosha Reveals Multiple Functions for miRNAs in Postnatal Skin. *Development* 139 (8), 1405–1416. doi:10.1242/dev.070920
- Tomann, P., Paus, R., Millar, S. E., Scheidereit, C., and Schmidt-Ullrich, R. (2016). LHX2 Is a Direct NF-Kb Target Gene that Promotes Primary Hair Follicle Placode Down-Growth. *Development* 143 (9), 1512–1522. doi:10.1242/dev.130898
- Vishlaghi, N., and Lisse, T. S. (2020). Dicer- and Bulge Stem Cell-dependent MicroRNAs during Induced Anagen Hair Follicle Development. *Front. Cell Dev. Biol.* 8, 338. doi:10.3389/fcell.2020.00338
- Wang, A. B., Zhang, Y. V., and Tumber, T. (2017a). Gata6 Promotes Hair Follicle Progenitor Cell Renewal by Genome Maintenance during Proliferation. *EMBO J.* 36 (1), 61–78. doi:10.15252/embj.201694572
- Wang, S., Ge, W., Luo, Z., Guo, Y., Jiao, B., Qu, L., et al. (2017b). Integrated Analysis of Coding Genes and Non-coding RNAs during Hair Follicle Cycle of Cashmere Goat (*Capra hircus*). *BMC Genomics* 18 (1), 767. doi:10.1186/s12864-017-4145-0
- Wu, Z., Wang, Y., Han, W., Yang, K., Hai, E., Ma, R., et al. (2020). EDA and EDAR Expression at Different Stages of Hair Follicle Development in Cashmere Goats and Effects on Expression of Related Genes. *Arch. Anim. Breed.* 63 (2), 461–470. doi:10.5194/aab-63-461-2020
- Yan, H., Tang, H., Qiu, W., Tan, R., Zhang, W., Yang, G., et al. (2019b). A New Dynamic Culture Device Suitable for Rat Skin Culture. *Cell Tissue Res.* 375 (3), 723–731. doi:10.1007/s00441-018-2945-4
- Yan, H., Gao, Y., Ding, Q., Liu, J., Li, Y., Jin, M., et al. (2019a). Exosomal MicroRNAs Derived from Dermal Papilla Cells Mediate Hair Follicle Stem Cell Proliferation and Differentiation. *Int. J. Biol. Sci.* 15 (7), 1368–1382. doi:10.7150/ijbs.33233
- Yi, R., O'Carroll, D., Pasolli, H. A., Zhang, Z., Dietrich, F. S., Tarakhovskiy, A., et al. (2006). Morphogenesis in Skin Is Governed by Discrete Sets of Differentially Expressed microRNAs. *Nat. Genet.* 38 (3), 356–362. doi:10.1038/ng1744
- Yi, R., Pasolli, H. A., Landthaler, M., Hafner, M., Ojo, T., Sheridan, R., et al. (2009). DGCR8-dependent microRNA Biogenesis Is Essential for Skin Development. *Proc. Natl. Acad. Sci. U.S.A.* 106 (2), 498–502. doi:10.1073/pnas.0810766105
- Yue, Y., Guo, T., Yuan, C., Liu, J., Guo, J., Feng, R., et al. (2016). Integrated Analysis of the Roles of Long Noncoding RNA and Coding RNA Expression in Sheep (*Ovis aries*) Skin during Initiation of Secondary Hair Follicle. *PLoS One* 11 (6), e0156890. doi:10.1371/journal.pone.0156890

- Zhang, Y., Tomann, P., Andl, T., Gallant, N. M., Huelsken, J., Jerchow, B., et al. (2009). Reciprocal Requirements for EDA/EDAR/NF- κ B and Wnt/ β -Catenin Signaling Pathways in Hair Follicle Induction. *Dev. Cell* 17 (1), 49–61. doi:10.1016/j.devcel.2009.05.011
- Zhao, B., Chen, Y., Yang, N., Chen, Q., Bao, Z., Liu, M., et al. (2019). miR-218-5p Regulates Skin and Hair Follicle Development through Wnt/ β -Catenin Signaling Pathway by Targeting SFRP2. *J. Cell. Physiology* 234 (11), 20329–20341. doi:10.1002/jcp.28633
- Zhao, R., Li, J., Liu, N., Li, H., Liu, L., Yang, F., et al. (2020). Transcriptomic Analysis Reveals the Involvement of lncRNA-miRNA-mRNA Networks in Hair Follicle Induction in Aohan Fine Wool Sheep Skin. *Front. Genet.* 11, 590. doi:10.3389/fgene.2020.00590
- Zhou, J., Zhang, X., Liang, P., Ren, L., Zeng, J., Zhang, M., et al. (2016). Protective Role of microRNA-29a in Denatured Dermis and Skin Fibroblast Cells after Thermal Injury. *Biol. Open* 5 (3), 211–219. doi:10.1242/bio.014910
- Zhou, L., Zhang, X., Paus, R., and Lu, Z. (2018). The Renaissance of Human Skin Organ Culture: A Critical Reappraisal. *Differentiation* 104, 22–35. doi:10.1016/j.diff.2018.10.002
- Zhu, N., Huang, K., Liu, Y., Zhang, H., Lin, E., Zeng, Y., et al. (2018/2018). miR-195-5p Regulates Hair Follicle Inductivity of Dermal Papilla Cells by Suppressing Wnt/ β -Catenin Activation. *BioMed Res. Int.* 2018, 1–13. doi:10.1155/2018/4924356
- Zhu, N., Lin, E., Zhang, H., Liu, Y., Cao, G., Fu, C., et al. (2020). LncRNA H19 Overexpression Activates Wnt Signaling to Maintain the Hair Follicle Regeneration Potential of Dermal Papilla Cells. *Front. Genet.* 11, 694. doi:10.3389/fgene.2020.00694

Conflict of Interest: The authors declare that the research was conducted in the absence of any commercial or financial relationships that could be construed as a potential conflict of interest.

Publisher's Note: All claims expressed in this article are solely those of the authors and do not necessarily represent those of their affiliated organizations, or those of the publisher, the editors and the reviewers. Any product that may be evaluated in this article, or claim that may be made by its manufacturer, is not guaranteed or endorsed by the publisher.

Copyright © 2022 Jiang, Liu, Zou, Li and Ding. This is an open-access article distributed under the terms of the Creative Commons Attribution License (CC BY). The use, distribution or reproduction in other forums is permitted, provided the original author(s) and the copyright owner(s) are credited and that the original publication in this journal is cited, in accordance with accepted academic practice. No use, distribution or reproduction is permitted which does not comply with these terms.